Available online at www.sciencedirect.com
ScienceDirect
Composites: Part A 38 (2007) 2047–2054
composites
Part A: applied science and manufacturing
www.elsevier.com/locate/compositesa

Comparison of different identification techniques for measurement of quasi-zero Poisson's ratio of fabric-reinforced laminates

I. De Baere [a,*], W. Van Paepegem [a], J. Degrieck [a], H. Sol [b], D. Van Hemelrijck [b], A. Petreli [b]

[a] Department of Mechanical Construction and Production, Sint-Pietersnieuwstraat 41, B-9000 Gent, Belgium
[b] Department Mechanics of Materials and Constructions (MEMC), Pleinlaan 2, B-1050 Brussel, Belgium

Received 14 December 2006; received in revised form 25 April 2007; accepted 25 April 2007

Abstract

The resonalyser method is a material identification technique which is based on the measurement of resonance frequencies of freely suspended rectangular test plates, combined with numerical simulations. By adjusting the ratio of the width to the length of the test plate, the resonance frequencies can be made very sensitive for small variations of Poisson's ratio. This study examines a fabric-reinforced composite material with a very small value of Poisson's ratio. The material on which the experiments are performed is a carbon fabric-reinforced polyphenylene sulphide. The accurateness of the determined values of the in-plane elastic properties of the test plates is validated with static tensile tests. First, the four orthotropic elastic properties, Young's moduli E_{11} and E_{22}, the in-plane shear modulus G_{12} and Poisson's ratio ν_{12}, are identified using the resonalyser technique. Next, the obtained values for Young's moduli and Poisson's ratio are validated with static uni-axial tests.

It can be concluded that the results derived from both measurement methods corresponded very well.

Keywords: A. Carbon fibre; A. Thermoplastic resin; B. Mechanical properties; D. Non-destructive testing

1. Introduction

When designing constructions with any type of material, the accurate knowledge of the elastic properties of the used materials is very important. Often, the choice of material and type of construction depend on it. Therefore, a large number of experiments are available to determine the various mechanical properties.

In this article, results from the so-called "resonalyser technique" [1,2] are compared with results obtained with simple uni-axial static tests for the determination of Young's modulus and Poisson's ratio for a material with a quasi-zero Poisson's ratio. The resonalyser method is a material identification technique which is based on the measurement of resonance frequencies of freely suspended rectangular test plates, combined with numerical simulations. It is an inverse method that identifies the material parameters in such a way that the numerically computed resonance frequencies match the experimental values. The results obtained with this method are then compared with the results from a standard tensile test according to the ASTM standard D3039-93 (standard test method for tensile properties of polymer matrix composite materials).

In the first paragraphs the theoretical background and the principle of the resonalyser is discussed. Then, the used material and test setups are presented. This is followed by the static tensile testing, in order to compare the results obtained with both methods. Finally, some conclusions are drawn concerning the correspondence between the values derived from both methods and on the effect of the quasi-zero Poisson's ratio on the expected mode shapes in the resonalyser technique.

* Corresponding author. Tel.: +32 09 264 32 55; fax: +32 09 264 35 87.
E-mail address: Ives.DeBaere@UGent.be (I. De Baere).

1359-835X/$ - see front matter © 2007 Elsevier Ltd. All rights reserved.
doi:10.1016/j.compositesa.2007.04.012

2. Theoretical background of the resonalyser

The elastic behaviour of materials having orthotropic symmetry axes in a state of plane stress can be described by the following relation between strains and stresses:

$$\begin{Bmatrix} \varepsilon_{11} \\ \varepsilon_{22} \\ \gamma_{12} \end{Bmatrix} = \begin{pmatrix} \frac{1}{E_{11}} & -\frac{\nu_{12}}{E_{11}} & 0 \\ -\frac{\nu_{21}}{E_{22}} & \frac{1}{E_{22}} & 0 \\ 0 & 0 & \frac{1}{G_{12}} \end{pmatrix} \begin{Bmatrix} \sigma_{11} \\ \sigma_{22} \\ \tau_{12} \end{Bmatrix} \quad (1)$$

In this expression, 1 and 2 are the main material axes of the orthotropic material, $(\varepsilon_{11}, \varepsilon_{22}, \gamma_{12})$ represents the strain components, $(\sigma_{11}, \sigma_{22}, \tau_{12})$ the stress components, E_{11} and E_{22} the Young's moduli in the first and second main material direction, ν_{12} and ν_{21} the Poisson's ratios and G_{12} is the shear modulus in the (1,2)-plane. If linear material behaviour is assumed, the elastic properties E_{11}, E_{22}, ν_{12}, ν_{21} and G_{12} are also called the 'engineering constants'. Since the compliance matrix in Eq. (1) is symmetric, only four independent engineering constants occur: E_{11}, E_{22}, ν_{12} and G_{12}.

The resonalyser procedure is a mixed numerical/experimental method that aims to identify the engineering constants of orthotropic materials using measured resonant frequencies of freely suspended rectangular specimens. For the identification of the four orthotropic material constants, it is necessary to measure the first three resonant frequencies of a rectangular plate and the first resonant frequency of two beams, one cut along the longitudinal direction and the other cut along the transversal direction of the test plate.

2.1. Identification of the Young's modulus by measuring the resonant frequency of a test beam

The first resonant frequency of a test beam with free boundary conditions is associated to a bending mode deformation. From the first resonance it is possible to calculate the Young's modulus E of the material in the longitudinal direction of the beam using the formula [3–6]:

$$E = 0.946 \frac{\rho f^2 L^4}{t^2} \ [\text{MPa}] \quad (2)$$

where, ρ: specific mass [kg/M^3]; f: measured resonant frequency [Hz]; t: thickness of the beam [mm]; L: length of the beam [mm].

This formula is only valid for sufficiently thin beams. This requires for composite materials a ratio L/t greater than 50.

2.2. Identification of the orthotropic stiffness properties by measuring the resonant frequencies of a test plate

The identification of the orthotropic stiffness properties is done by simulation of the rectangular test plate using a numerical model on the computer. The numerical model allows the calculation of the resonant frequencies on the condition that the stiffness properties, the dimensions and the mass of the plate are known. The basic principle of the resonalyser is to compare measured frequencies of the test plate with computed frequencies using a numerical finite element model of the same test plate (Fig. 1). The engineering constants in the numerical model are considered as unknown material parameters. Starting from an initial guess, the engineering constants are iteratively updated till a series of numerically computed resonance frequencies match the experimentally measured frequencies.

Such an inverse procedure can only yield good results if the numerical model is controllable and if the elastic properties can be observed through the measured data [7–9]. This requires that in the selected series of frequencies at least one of the frequencies varies significantly for variations of each of the elastic properties. It can be shown [10,11] that this requirement is fulfilled if the ratio a/b of the length and width of the test plate equals approximately to $\frac{a}{b} = \sqrt{\frac{E_{11}}{E_{22}}}$. A plate with such a ratio is called a 'Poisson test plate' [11]. A Poisson test plate shows a predictable sequence of mode shapes for the first 3 resonances: a torsional, an anticlastic and a synclastic (Fig. 2). The anticlastic mode is also known as the saddle mode and the synclastic is known as the breathing mode.

The name 'Poisson test plate' has been chosen based on the observation that the frequencies of the anticlastic and synclastic mode shapes are particularly sensitive for changes of the Poisson's ratio of the plate material. A material with a (hypothetical) zero value for Poisson's ratio would make the frequencies of both modes coincide, which means that the synclastic and anticlastic modes become pure bending modes in respectively the 1 and the 2-direction. The values E_{11} and E_{22} necessary to compute the plate sizes a and b can be found by cutting two test beams, one along the first principal material direction and a second along the second principal direction. By measuring the first resonance frequencies of the freely suspended test beams, the values of E_{11} and E_{22} can be computed using formula (2). The obtained values of E_{11} and E_{22} are also used as initial values for the resonalyser procedure. Good initial values for the other elastic constants G_{12} and ν_{12} can be obtained with empirical formulas [11]. The determination

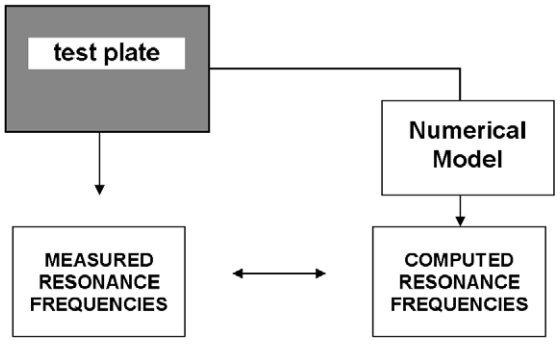

Fig. 1. Comparison between experimentally measured and computed resonance frequencies of the same test plate.

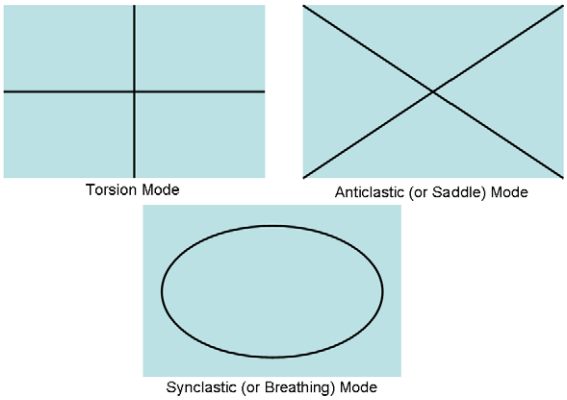

Fig. 2. The first three mode shapes of a Poisson test plate.

of these values will be discussed in Section 2.3. Starting with these initial values, the engineering constants in a finite element model of the test plate are iteratively updated till the three first computed resonance frequencies match the measured frequencies associated with the mode shapes shown in Fig. 2. In the finite element model, the plate dimensions and mass are considered as known and fixed values. The four engineering constants are stored in a parameter column p. The updating of p is realised by minimising a cost function $C(p)$:

$$C(p) = (m_r - y_r(p)) \cdot W^m_{rs} \cdot (m_s - y_s(p)) + (p^{(0)}_r - p_r) \cdot W^m_{rs} \cdot (p^{(0)}_s - p_s) \quad (3)$$

In Eq. (3) $C(p)$ is a $\Re^{NP} \rightarrow \Re$ cost function yielding a scalar value, p is a $(NP \times 1)$ column containing the $NP = 4$ material parameters E_{11}, E_{22}, v_{12} and G_{12}, $\{p^{(0)}\}$ contains the initial estimates for the material parameters, $\{y\}$ is a $(NP \times 1)$ output column containing the $NM = 3$ computed frequencies using parameter values $\{p\}$, $\{m\}$ contains the $(NP \times 1)$ measured frequencies, $[W^{(m)}]$ is a $(NP \times NM)$ weighing matrix applied on the difference between the measured column and the output column, and $[W^{(p)}]$ is a $(NP \times NP)$ weighing matrix for the difference between the initial parameter column $\{p^{(0)}\}$ and the parameter column $\{p\}$.

The cost function $C(p)$ has a minimal value for the optimal parameter values column $\{p^{(opt)}\}$. The choice of the weighting matrices is discussed, among others, in [7,12,13] The updating of the initial parameter column toward $\{p^{(opt)}\}$ by minimization of the cost function is given by the following recurrence formula in iteration step $(j+1)$:

$$p^{(j+1)}_k = p^{(j)}_k + [W^p_{km} + S^j_{rk} \cdot W^{(m)}_{rs} \cdot S^j_{sm}]^{-1} \cdot (S^j_{rm} \cdot W^{(m)}_{rs} \cdot (m_s - y^{(j)}_s) + W^{(p)}_{ms} \cdot (p^{(0)}_s - p^{(j)}_s)) \quad (4)$$

In Eq. (4) S^j is the sensitivity matrix containing the partial derivatives of the output column to the parameter column.

The measurement of the three resonance frequencies of the test plate can be performed simple, fast and accurate with a PC equipped with a data acquisition card. An accelerometer is fixed on the freely suspended test plate which is impacted with a small hammer. The generated time domain signal in the accelerometer is digitised by the data acquisition card and stored in the computer's memory. Next the signal is transformed by a Fast Fourier Transformation [14] to the frequency domain in which the resonance frequencies occur as sharp peaks and can easily be identified. The numerical model of the test plate is based on the Love–Kirchhoff theory for thin plates. The model is sufficiently accurate if the length/thickness ratio of the plate exceeds a factor of about 50 [15]. Very accurate eight order polynomial Lagrange functions are taken as the shape functions in the used numerical finite element model of the test plate [11]. The stiffness matrix of the test plate is evaluated in each iteration cycle using standard finite element procedures with the values of the parameter column p at that moment. The computed resonance frequencies are obtained by the solution of a generalised eigenvalue problem composed with the constant mass matrix and the evaluated stiffness matrix. The iteration procedure using Eq. (4) ends if convergence of p is reached. The value of the engineering constants in p in the last iteration cycle is considered as the result of the resonalyser procedure.

2.3. Determination of the initial values of the orthotropic stiffness properties used by the numerical model

The measurement of the resonant frequencies of two test beams (which was necessary to establish the correct test plate ratio), also supplies us with good initial values of E_{11} and E_{22}, via the formula (2).

For the determination of the initial values of the Poisson ratio and the shear modulus G_{12}, we need a further study of the mode shapes of the rectangular plate. As mentioned above (Fig. 2), the first mode of the test plate is a torsion mode. The magnitude of the eigenvalue belonging to this mode is almost exclusively determined by the shear modulus G_{12}, and can be approximated by the formula [11]:

$$\lambda_T = 41.75 \frac{G_{12} t^3}{Mab} \quad (5)$$

where $\lambda = (2\pi f_T)^2$: eigenvalue corresponding to the torsion mode [Hz^2]; t: thickness of the test plate [mm]; f_T: resonant frequency corresponding to the torsion mode [Hz]; b: width of the test plate [mm]; a: length of the test plate [mm]; M: mass of the test plate [kg].

The eigenvalues belonging to the saddle and breathing modes coincide when the Poisson ratio is equal to zero. A value of Poisson's ratio different from zero makes the eigenvalue of the saddle mode decrease and the eigenvalue of the breathing mode increase. So, the bigger the Poisson's ratio, the bigger becomes the difference between the eigenvalues of the saddle and breathing modes. Using an empirical formula it is possible to express the relation between the Poisson's ratio and the two eigenvalues [10,11]:

$$v_{12} = C_1 \frac{\lambda_A - \lambda_Z}{\lambda_A + \lambda_Z} \quad (6)$$

where $\lambda_A = (2\pi f_A)^2$: eigenvalue corresponding to the breathing mode [Hz^2]; $\lambda_Z = (2\pi f_Z)^2$: eigenvalue corresponding to the saddle mode [Hz^2]; f_A: resonant frequency corresponding to the breathing mode [Hz]; f_Z: resonant frequency corresponding to the saddle mode [Hz]; C_1: a constant [–].

3. Material and experimental setup

3.1. Material

The material under study was a carbon fibre-reinforced polyphenylene sulphide (PPS), called CETEX. This material is supplied by Ten Cate. The fibre type is the carbon fibre T300J 3 K and the weaving pattern is a 5-harness satin weave with a mass per surface unit of 286 g/m^2. The 5-harness satin weave is a fabric with high strength in both directions and excellent bending properties.

The carbon PPS plates were hot pressed and two stacking sequences were used for this study, namely a $[\#0°]_{4s}$ and a $[\#0°/\#90°]_{2s}$ were (#0°) represents one layer of fabric.

The thickness of each layer is about 0.3 mm, the density of the lamina is 1555 kg/m^3 and the fibre volume fraction is 50%.

For the resonalyser method, two different test plates were used:

Plate 1: $[\#0°]_{4s}$
The warp direction of all the 8 layers coincides (the weft direction is perpendicular to the warp). One plate and 8 beams (4 along the warp and 4 along the weft direction) were cut out of the master plate.
Plate 2: $[\#0°/\#90°]_{2s}$
The warp direction of each layer is 0° and 90° alternatively, starting with the warp direction at the upper layer. Again, one test plate and 8 test beams (4 along the warp and 4 along the weft direction) were cut.

The exact geometry, mass and specific mass of each test specimen are given in Table 1.

For the static testing, only the $[\#0°]_{4s}$ was used. The test coupons were sawn with a water-cooled diamond saw, the dimensions of the coupons are shown in Fig. 3. $[\pm45°]_{2s}$ glass fibre epoxy tabs were used in order to avoid damage of the specimens by the grips of the tensile machine.

An example of an instrumented tensile coupon is depicted in Fig. 4.

3.2. Experimental setup for the resonalyser method

The experimental setup includes a suspension frame for the rectangular test plate, a loudspeaker for the excitation, a laser velocity vibrometer, a signal conditioning unit, a data acquisition unit and a personal computer (see Fig. 5).

The test plate is suspended on the frame with thin strings. This configuration simulates completely free

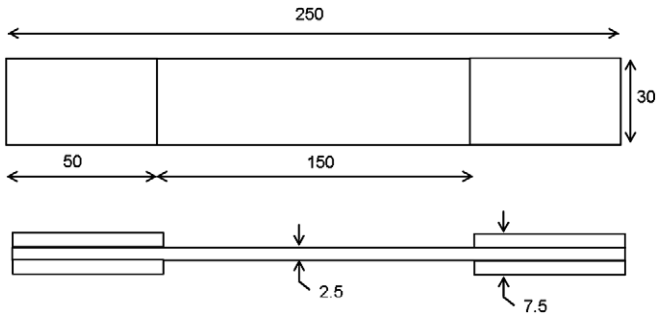

Fig. 3. Dimensions of the used tensile coupon, equipped with tabs of $[\pm45°]_{2s}$ glass fibre epoxy.

Table 1
Geometry, mass and specific mass of the test specimens

Specimen	Length [m]	Width [m]	Thickness [m]	Mass [kg]	Specific mass [kg/m^3]
Plate $[\#0°]_8$	0.149	0.14904	0.00241	0.08350	1560.200
Plate $[\#0°/\#90°]_{2s}$	0.14934	0.14993	0.00241	0.08314	1543.939
Beam 1: $[\#0°]_8$	0.1488	0.02153	0.00235	0.01189	1579.309
Beam 2: $[\#0°]_8$	0.1482	0.0222	0.00241	0.01238	1561.358
Beam 3: $[\#0°]_8$	0.14854	0.0234	0.00237	0.01290	1565.965
Beam 4: $[\#0°]_8$	0.14904	0.0235	0.00239	0.01319	1575.710
Beam 5: $[\#90°]_8$	0.14823	0.02365	0.00242	0.01305	1538.253
Beam 6: $[\#90°]_8$	0.14875	0.02288	0.00236	0.01269	1579.926
Beam 7: $[\#90°]_8$	0.14848	0.02405	0.00236	0.01329	1576.994
Beam 8: $[\#90°]_8$	0.14809	0.02346	0.00238	0.01308	1581.893
Beam 9: $[\#0°/\#90°]_{2s}$	0.14948	0.02207	0.00241	0.01237	1555.848
Beam 10: $[\#0°/\#90°]_{2s}$	0.14936	0.02409	0.00240	0.01340	1551.752
Beam 11: $[\#0°/\#90°]_{2s}$	0.14926	0.02315	0.00242	0.01283	1534.323
Beam 12: $[\#0°/\#90°]_{2s}$	0.14915	0.02341	0.00243	0.01304	1536.904
Beam 13: $[\#0°/\#90°]_{2s}$	0.14913	0.02320	0.00239	0.01286	1555.214
Beam 14: $[\#0°/\#90°]_{2s}$	0.14926	0.02355	0.00239	0.01297	1543.859
Beam 15: $[\#0°/\#90°]_{2s}$	0.14941	0.023	0.00236	0.01271	1567.206
Beam 16: $[\#0°/\#90°]_{2s}$	0.149	0.02349	0.00239	0.01300	1554.090

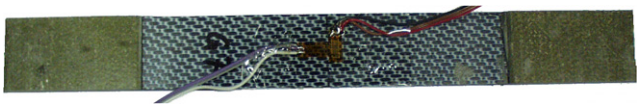

Fig. 4. An example of a specimen instrumented with the longitudinal and transverse strain gauge.

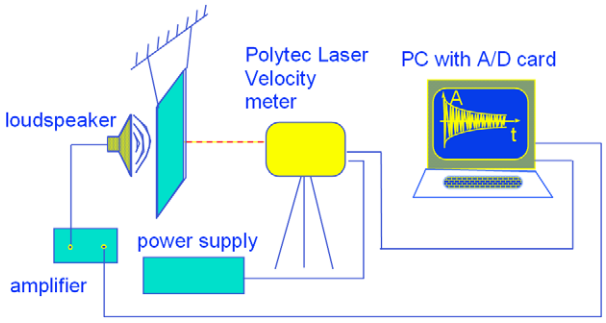

Fig. 5. The resonalyser setup.

boundary conditions. The test plate is excited by a periodic chirp signal with a desired bandwidth through a loudspeaker. As a result of this excitation, the test plate will start to vibrate on its resonance frequencies inside the frequency band of the signal. The vibration amplitude of the plate as a function of time is picked up by the laser vibrometer and stored in the memory of PC by a data acquisition system. The resonance frequencies of the plate in the band of interest are detected by taking the Fast Fourier transform of the signal.

3.3. Experimental setup for the static tests

All tensile tests were performed on a servo-hydraulic INSTRON 1342 tensile testing machine with a FastTrack 8800 digital controller and a load cell of ±100 kN. The tests were displacement-controlled with a speed of 2 mm/min.

The strain gauges were mounted in the 0° and 90° directions to measure longitudinal and transverse strain. Poisson's ratio is then given by

$$v_{12} = -\frac{\varepsilon_{22}}{\varepsilon_{11}} \tag{7}$$

For the registration of the data, a combination of a National Instruments DAQpad 6052E for fireWire, IEEE 1394 and the SCB-68 pin shielded connecter were used. The load, displacement and strain, given by the FastTrack controller, as well as the extra signals from strain gauges were sampled on the same time basis. The latter is necessary to be able to calculate Poisson's ratio.

4. Results

4.1. Identification of the material properties using the resonalyser procedure

The first three resonant frequencies of the plates, as well as the first resonance of each beam were measured with the setup. Next the material properties in the numerical model in the resonalyser procedure were tuned iteratively, as described in Section 2, till the computed frequencies match the measured frequencies as closely as possible. The values

Table 2
Measured resonant frequencies using accelerometer and identified material properties via the resonalyser technique

Specimen	Resonant frequency [Hz]	E_{11} [GPa]	E_{22} [GPa]	G_{12} [GPa]	v_{12} [–]
Plate $[\#0°]_8$	201.96 625.91 687.02	61.8	50.8	4.82	0.023
Plate $[\#0°/\#90°]_{2s}$	193.49 636.87 660.34	56.9	56.7	4.48	0.040
Beam 1: $[\#0°]_8$	662.08	58.14	–	–	–
Beam 2: $[\#0°]_8$	666.15	54.44	–	–	–
Beam 3: $[\#0°]_8$	666.52	57.04	–	–	–
Beam 4: $[\#0°]_8$	664.42	56.84	–	–	–
Beam 5: $[\#90°]_8$	616.05	–	45.53	–	–
Beam 6: $[\#90°]_8$	607.06	–	48.42	–	–
Beam 7: $[\#90°]_8$	612.11	–	48.78	–	–
Beam 8: $[\#90°]_8$	617.34	–	48.42	–	–
Beam 9: $[\#0°/\#90°]_{2s}$	641.11	52.00	–	–	–
Beam 10: $[\#0°/\#90°]_{2s}$	643.09	52.45	–	–	–
Beam 11: $[\#0°/\#90°]_{2s}$	639.38	50.29	–	–	–
Beam 12: $[\#0°/\#90°]_{2s}$	644.22	50.57	–	–	–
Beam 13: $[\#0°/\#90°]_{2s}$	637.92	–	51.84	–	–
Beam 14: $[\#0°/\#90°]_{2s}$	634.03	–	51.01	–	–
Beam 15: $[\#0°/\#90°]_{2s}$	631.29	–	52.87	–	–
Beam 16: $[\#0°/\#90°]_{2s}$	634.52	–	51.07	–	–

Fig. 6. Bending mode of a typical test beam.

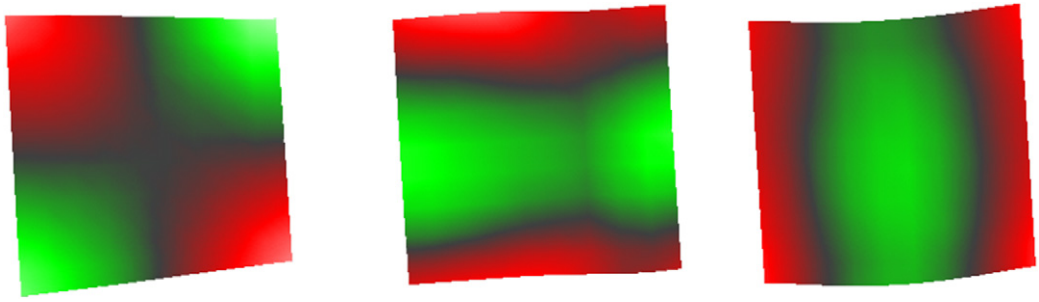

Fig. 7. Mode shapes of plate 1: $[\#0°]_{4s}$ corresponding to the first three resonant frequencies, measured with the laser velocity vibrometer.

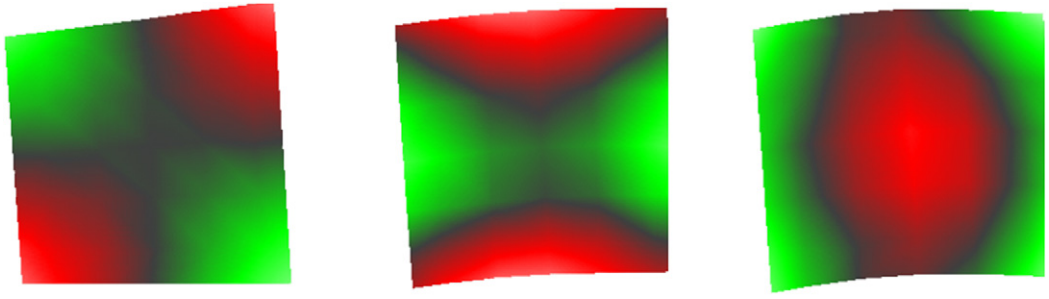

Fig. 8. Mode shapes of plate 2: $[\#0°/\#90°]_{2s}$ corresponding to the first three resonant frequencies, measured with the laser velocity vibrometer.

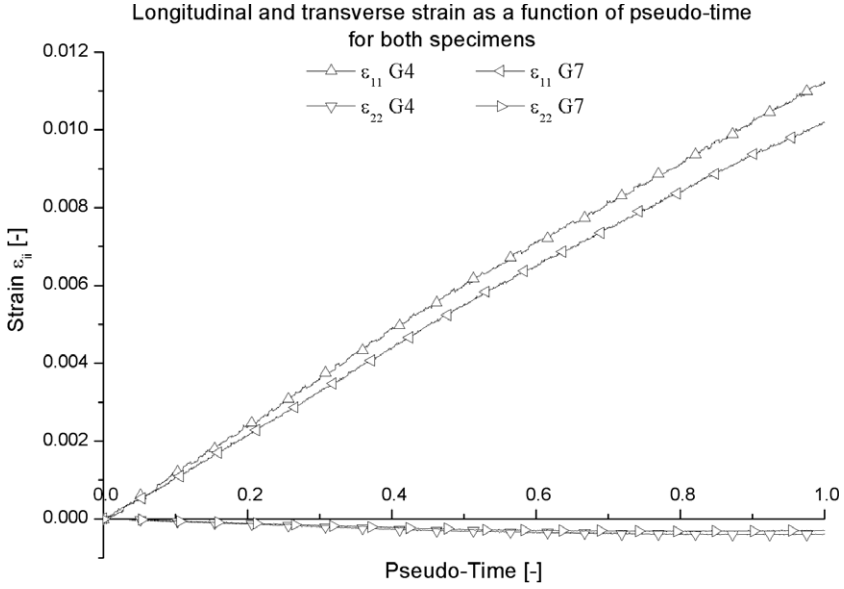

Fig. 9. ε_{11} and ε_{22} as a function of pseudo-time for both specimens.

of the four orthotropic stiffness properties in the last iteration cycle of this procedure were identified, and the final results are listed in Table 2.

The values of E_{11} and E_{22} measured from the resonance frequencies of the beam specimens using formula (2) is also listed in Table 2.

4.2. Visualisation of the mode shapes

The mode shapes of a typical test beam and the mode shapes of both test plates are visualised using a laser vibrometer.

The mode shapes corresponding to the measured resonant frequencies for the beam is given in Fig. 6 and those for both plates are given in Figs. 7 and 8. For the latter, it can be noticed that the synclastic and anticlastic mode (second and third mode) are very much alike and are practically bending modes.

4.3. Static tensile test results

Fig. 9 gives the evolution of both longitudinal and transverse strains for both the $[\#0°]_{4s}$ specimens G4 and G7 as a function of pseudo-time, where 0 corresponds with the start of the experiment and 1 corresponds with failure of the specimen. It can be noticed that the transverse strains remain very small. At failure they reach a value of -0.00039 for G4 and -0.00030 for G7. The ultimate

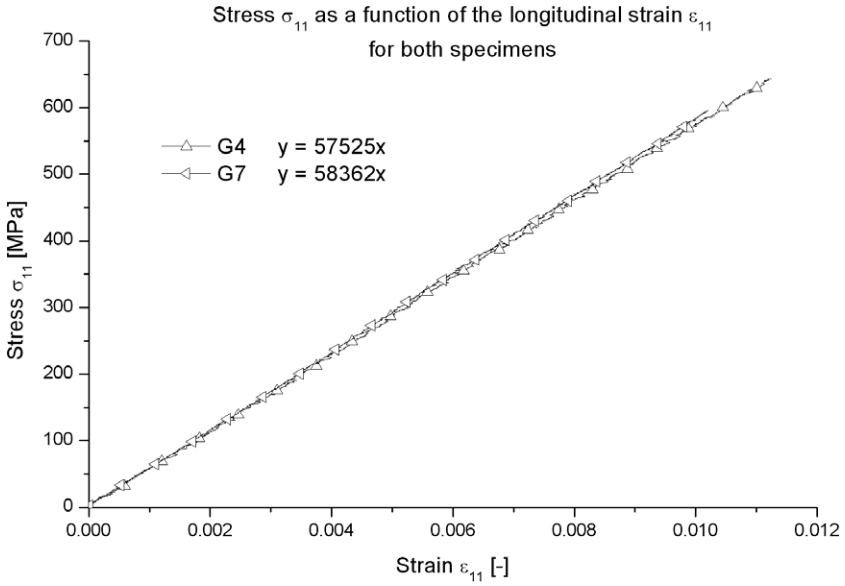

Fig. 10. σ_{11} as a function of ε_{11} for both specimens.

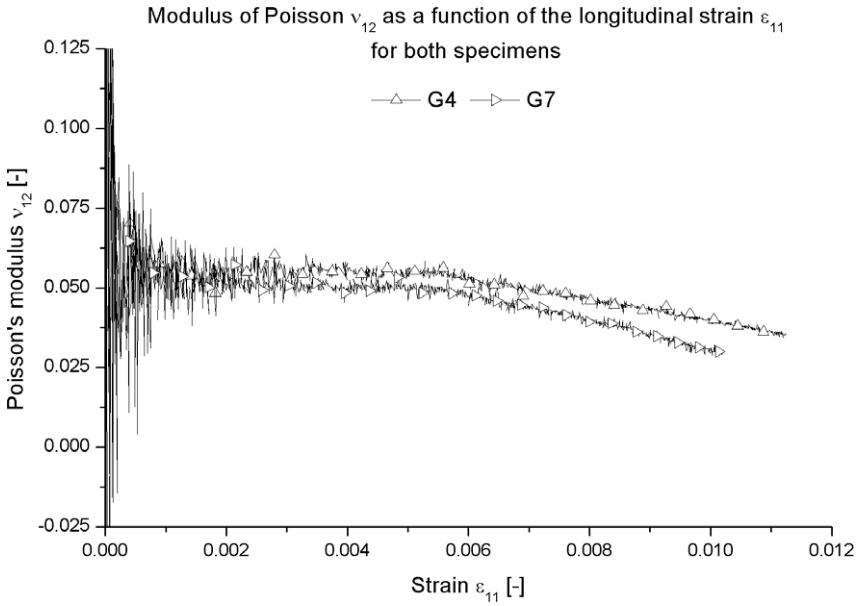

Fig. 11. ν_{12} as a function of ε_{11} for both specimens.

longitudinal strains are 0.0112 and 0.0102, respectively, for G4 and G7.

In Fig. 10, the evolution of the stress σ_{11} as a function of the strain ε_{11} is given. It may be concluded that this material has a linear behaviour up to failure. The failure stresses are 643.5 MPa for G4 and 594.3 MPa for G7. Young's modulus can also be derived from these experiments, a value of 57.5 GPa for G4 and 58.4 GPa for G7 are found. These values show good agreement with the values in Table 2.

Finally, Fig. 11 shows the evolution of Poisson's ratio as a function of the longitudinal strain. An average value of 0.049 and 0.053 is found for G4, respectively, G7. This value also shows good correspondence with the values found with the resonalyser technique (Table 2).

It must be remarked that the value of ν_{12} is very low, considering the fact that the fibre-reinforcement is a fabric. Normally, values between 0.2 and 0.4 are found [16,17]. However, a similar low value was found by Hofstee et al. [18] for a similar material.

It may also be noted that once the longitudinal strain exceeds about 0.006, the ratio tends to decrease. At fracture, ν_{12} is only about 60% of its original value, namely 0.035 for G4 and 0.03 for G7. This decrease in the Poisson's ratio may present the possibility to use ν_{12} as a means to characterize damage. However, further research and experiments are necessary in order to prove this.

5. Conclusions

The resonalyser technique is well suited for the accurate identification of the elastic properties of an orthotropic composite material. The values determined with this method show good correspondence with the values derived from the static uni-axial tests. However, the advantage of the resonalyser technique over the uni-axial test is the little preparation time needed for the experiments, once the resonalyser setup is acquired, since the technique does not require strain gauges, extensometers or end tabs.

The Poisson's ratio of the plate $[\#0°]_{4s}$ is very small. An average value of 0.052 was found. For the resonalyser technique, this causes the second and third mode shapes to be two bending mode shapes instead of saddle and breathing mode shapes. The low ν_{12} is also confirmed by the $[\#0°/\#90°]_{2s}$.

When considering the evolution of Poisson's ratio, a clearly decreasing trend is noticed. This should allow the use of ν_{12} as a way to characterize damage in the material. However, further research on this matter is necessary.

Acknowledgements

The authors are highly indebted to the university research fund BOF (Bijzonder Onderzoeksfonds UGent) for sponsoring this research and Ten Cate advanced composites for supplying the material. The authors also thank the FWO (Fonds Wetenschappelijk Onderzoek) for the financial support.

References

[1] Sol H, Hua H, De Visscher J, Vantomme J, De Wilde WP. A mixed numerical/experimental technique for the nondestructive identification of the stiffness properties of fibre reinforced composite materials. J NDT&E Int 1997;30(2):85–91.
[2] Lauwagie T, Sol H, Roebben G, Heylen W, Shi Y. Validation of the resonalyser method: an inverse method for material identification. In: Proceedings of ISMA 2002, international conference on noise and vibration engineering, Leuven, 16–18 September, 2002, p. 687–94.
[3] Förster F. Ein neues Messverfahren zur Bestimmung des Elastizitätsmoduls und der Dämpfung. Z Metallkd 1937;29:109–15.
[4] Pickett G. Equations for computing elastic constants from flexural and torsional resonant frequencies of vibrating prisms and cylinders. Proc ASTM 1945;45:846–65.
[5] Spinner S, Teft WE. A method for determining mechanical resonance frequencies and for calculating elastic moduli from these frequencies. Proc ASTM 1961;61:1209–21.
[6] Sol H, Lauwagie T, Heylen W, Roebben G. Simultaneous identification of the elastic and damping properties of composite materials as a function of temperature. Second International workshop on damping technologies, Materials and devices for the next decade, Stellenbosch, South Africa, 24–26 March, 2003.
[7] Hua H. Identification of plate rigidities of anisotropic rectangular plates, Sandwich Panels and orthotropic circular disks using vibration data. PhD thesis presented at the Vrije Universiteit Brussel Belgium,1993.
[8] Kreindler E, Sarachik PE. On the concepts of controllability and observability of linear systems. IEEE trans A C 1964;AC-9.
[9] Lauwagie, T, Heylen, W. A multi-model updating routine for layered material identification, In: Proceedings of the international modal analysis conference, IMAC XXI, Kissimmee, 3–6 February, 2003.
[10] Sol H et al. La procedure resonalyser. La revue des laboratoires d'Essais 1996;46:10–2.
[11] Sol H. Identification of anisotropic plate rigidities using free vibration data, PhD thesis presented at the vrije Universiteit Brussel, Belgium, 1986.
[12] Collins JD, Hart GC, Hasselman TK, Kennedy B. Statistical identification of structures. AIAA J 1974;12(2):185–90.
[13] Sol H, Oomens C. Material identification using mixed numerical experimental methods. Kluwer Academic Publishers; 1997.
[14] Brigham E Oren. The fast fourier transform and its applications. Englewood Cliffs, NJ: Prentice-Hall; 1988, p. 448.
[15] Vinson Jack R. Plate and panel structures of isotropic, composite and piezoelectric materials, including sandwich construction. Solid mechanics and its applications, vol. 120. Springer; 2005.
[16] Gommers B, Verpoest I, VanHoutte P. Modelling the elastic properties of knitted-fabric-reinforced composites. Compos Sci Technol 1996;56(6):685–94.
[17] Sun HY, Pan N, Postle R. On the Poisson's ratios of a woven fabric. Compos Struct 2005;68(4):505–10.
[18] Hofstee J, de Boer H, van Keulen F. Elastic stiffness analysis of a thermo-formed plain-weave fabric composite – part III: experimental verification. Compos Sci Technol 2002;62(3):401–18.